

Effective algorithms for tensor train decomposition via the UTV framework

Yuchao Wang, Maolin Che, and Yimin Wei

Abstract—The tensor train (TT) decomposition is used to compress large tensors into a more compact form by exploiting their inherent data structures. A fundamental approach for constructing the TT format is the TT-SVD, which extracts the TT-cores by the singular value decompositions (SVDs) sequentially. But in practical applications, it is often not necessary to compute full SVDs. In this article, we therefore propose a new method called the TT-UTV. It utilizes the virtues of rank-revealing UTV decomposition to compute the TT format for a large-scale tensor, hence requires less computational cost. We analyze the error bounds on the accuracy of these algorithms both in the URV and ULV cases, then recommend different sweep patterns for these two cases. We perform numerical experiments on some applications, including magnetic resonance imaging (MRI) data completion, to illustrate their good performance in practice.

Index Terms—Tensor train decomposition, UTV decomposition, tensor completion.

I. INTRODUCTION

REAL-WORLD high-dimensional data are usually represented as tensors, such as genetic analysis, video sequences, hypergraphs, hyperspectral images, and social network interactions [14], [23], [5], [41], [21]. Tensors provide a natural way to model multi-dimensional data and multi-modal nonlinear interactions. Due to the “curse of dimensionality” [15], direct usage of these higher-order tensors requires a lot of resources as the time and space complexity grow exponentially with the order of the tensor. Fortunately, tensors in the real world often have low-rank structure and the tensor-train decomposition [29], [28], also well-known as matrix product state representation [30], can exploit the inherent low-rank structure to mitigate the curse of dimensionality in many practical scenarios.

The tensor train (TT) decomposition has found widespread applications in areas such as machine learning [44], [27], [34], quantum many-body physics [32], signal processing [33], data completion [35], [2] and numerical partial differential equations [8], [31]. For a d th-order tensor, the TT-SVD algorithm [29] sequentially utilizes $d - 1$ singular value decompositions to extract core tensors one by one, which

becomes a foundational approach to decompose a higher-order tensor into the TT format.

In many circumstances, the SVD is computationally demanding and difficult to update, which gives birth to the UTV decomposition [36]. It provides approximately the same numerical rank and subspace information compared to SVD, while maintaining significantly lower computational cost [36], [10], [9], [7]. Moreover, UTV decomposition can be implemented to achieve higher performance on modern hardware architectures by leveraging block matrix operations, which are well suited for parallel processing [26]. Due to its virtues, UTV decomposition becomes a common alternative for SVD in many applications including signal processing and machine learning [43], [45]. Recently, the UTV decomposition is also extended to the decompositions for higher-order tensors. For example, a truncated multilinear UTV decomposition [39] is introduced for tensors from the truncated multilinear SVD [6], [40], the t-UTV decomposition [4] is proposed for third-order tensors as a substitute to the t-SVD based on the t-product [17].

In this article, we investigate whether the UTV decomposition can be leveraged to construct the TT decomposition, as economic alternatives to the TT-SVD. The goal is to save the computational cost by utilizing the advantages of UTV decomposition over SVD. Hence, a variety of algorithms for UTV decomposition can be employed for TT decomposition. This new approach is called TT-UTV. There exist two types of TT-UTV algorithms, corresponding to the URV and ULV cases, respectively. We provide an in-depth error analysis for these algorithms and demonstrate their effectiveness through various numerical experiments including image compression and MRI data completion.

This paper is organized as follows. We report the involved notions in Section 2. In Section 3, we introduce the TT-ULV algorithm in left-to-right sweep and TT-URV algorithm in right-to-left sweep, respectively, and derive rigorous error bounds for them, which explain how the UTV decompositions are utilized to achieve accurate and efficient tensor-train decomposition. In Section 4, we conduct extensive performance evaluations of the TT-UTV algorithm with TT-SVD in various applications.

II. RELATED WORKS

Notations. A d th-order tensor is a multidimensional array with d free indices, matrices are second-order tensors and vectors are first-order tensors. We mainly inherit the usage of notations from the comprehensive works of Kolda et al.

This paragraph of the first footnote will contain the date on which you submitted your paper for review. It will also contain support information, including sponsor and financial support acknowledgment.

Yuchao Wang is with the the School of Mathematical Sciences, Fudan University, Shanghai, 200433, P. R. China (e-mail: yuchaowang21@m.fudan.edu.cn).

Maolin Che is with School of Mathematics and Statistics, Guizhou University, Guiyang, 550025, P. R. of China (e-mail: chnclm@outlook.com).

Yimin Wei is with School of Mathematical Sciences and Key Laboratory of Mathematics for Nonlinear Sciences, Fudan University, Shanghai, 200433, P. R. China (e-mail: ymwei@fudan.edu.cn)

[20]. The calligraphic capital letters such as \mathcal{A} , boldface capital letters such as \mathbf{A} , and boldface lowercase letters such as \mathbf{a} are used to denote the tensors, matrices, and vectors, respectively. $\mathbb{R}^{I_1 \times \dots \times I_d}$ denotes the set of all d th-order tensors of dimensions (I_1, \dots, I_d) over the real number field \mathbb{R} , where I_k is the dimension of the k th mode of the tensor. The entries of $\mathcal{A} \in \mathbb{C}^{I_1 \times \dots \times I_d}$ are accessed by $\mathcal{A}_{i_1 i_2 \dots i_d}$ or $\mathcal{A}(i_1, i_2, \dots, i_d)$ for $1 \leq i_k \leq I_k$. For a tensor \mathcal{A} , we denote by \mathbf{A}_k its k th unfolding matrix.

A. Tensor basics

Tensor unfolding, the process of rearranging the elements of a tensor into a matrix or vector, is a frequently used operation in tensor analysis and numerical computations [1], [20]. The reverse lexicographic ordering (as the ‘reshape’ command in MATLAB) is one of the most commonly used approaches for integrating multiple indices into a single long index. Concretely, for the tensor dimensions $\mathbf{I} = (I_1, \dots, I_d)$ and a corresponding index vector $\mathbf{i} = (i_1, \dots, i_d)$, define the index mapping

$$\text{ivec}(\mathbf{i}, \mathbf{I}) := i_1 + \sum_{k=2}^d (i_k - 1) \prod_{j=1}^{k-1} I_j.$$

Definition II.1 (The k th unfolding matrix [29]). For a d th order tensor $\mathcal{A} \in \mathbb{R}^{I_1 \times \dots \times I_d}$, the matrix $\mathbf{A}_k \in \mathbb{R}^{(I_1 \dots I_k) \times (I_{k+1} \dots I_d)}$ is called the k th unfolding matrix of \mathcal{A} such that

$$\mathbf{A}_k(i, j) = \mathcal{A}_{i_1 \dots i_k i_{k+1} \dots i_d},$$

where $i = \text{ivec}((i_1, \dots, i_k), (I_1, \dots, I_k))$ and $j = \text{ivec}((i_{k+1}, \dots, i_d), (I_{k+1}, \dots, I_d))$.

The tensor train (TT) decomposition represents a higher-order tensor $\mathcal{A} \in \mathbb{R}^{I_1 \times \dots \times I_d}$ as the contractions of small factor tensors

$$\mathcal{A}_{i_1 \dots i_d} = \sum_{\alpha_0=1}^{r_0} \sum_{\alpha_1=1}^{r_1} \dots \sum_{\alpha_d=1}^{r_d} \mathcal{G}_{\alpha_0 i_1 \alpha_1}^{(1)} \mathcal{G}_{\alpha_1 i_2 \alpha_2}^{(2)} \dots \mathcal{G}_{\alpha_{d-1} i_d \alpha_d}^{(d)}, \quad (1)$$

where $r_0 = r_d = 1$, these third-order tensors $\mathcal{G}^{(k)} \in \mathbb{C}^{r_{k-1} \times I_k \times r_k}$ for $k = 1, 2, \dots, d$ are called TT-cores, and $(r_1, r_2, \dots, r_{d-1})$ are TT-ranks. The TT-SVD algorithm computes the tensor format (1) with left-orthogonal cores by a single left-to-right sweep or right-orthogonal cores by a right-to-left sweep; more details can be found in [29].

Definition II.2 (Orthogonal cores[29]). The cores $\{\mathcal{G}^{(k)}\}_{k=1}^d$ in (1) are called left-orthogonal if

$$\mathbf{G}_2^{(k)\top} \mathbf{G}_2^{(k)} = \mathbf{I}_{r_k},$$

where $\mathbf{G}_2^{(k)} \in \mathbb{R}^{r_{k-1} I_k \times r_k}$ are the second unfolding matrices of the TT-cores $\mathcal{G}^{(k)}$. They are right-orthogonal if

$$\mathbf{G}_1^{(k)} \mathbf{G}_1^{(k)\top} = \mathbf{I}_{r_{k-1}}$$

where $\mathbf{G}_1^{(k)} \in \mathbb{R}^{r_{k-1} \times I_k r_k}$ are the first unfolding matrices of the TT-cores $\mathcal{G}^{(k)}$.

Definition II.3 (Mode product [20]). The mode- k product of $\mathcal{X} \in \mathbb{C}^{I_1 \times \dots \times I_d}$ with a matrix $\mathbf{A} \in \mathbb{C}^{J \times I_k}$ is an $I_1 \times \dots \times I_{k-1} \times J \times I_{k+1} \times \dots \times I_d$ tensor, given by

$$(\mathcal{X} \times_k \mathbf{A})_{i_1 \dots i_{k-1} j i_{k+1} \dots i_d} = \sum_{i_k=1}^{I_k} \mathcal{X}_{i_1 \dots i_{k-1} i_k i_{k+1} \dots i_d} \mathbf{A}_{j i_k}.$$

Apart from the tensor-train decomposition, the Tucker format [38] is another compact form for larger-scale tensors, which represents a d th-order tensor via the mode products of a smaller-scaled core tensor and d factor matrices:

$$\mathcal{A} = \mathcal{S} \times_1 \mathbf{U}_1 \times_2 \dots \times_d \mathbf{U}_d, \quad (2)$$

where $\mathcal{S} \in \mathbb{R}^{r_1 \times \dots \times r_d}$ and $\mathbf{U}_k \in \mathbb{R}^{I_k \times r_k}$ for $1 \leq k \leq d$. Directly from these definitions, we can derive the following proposition.

Proposition II.1. Let the tensor \mathcal{A} be given in the Tucker format (2). Then the k th unfolding matrices \mathbf{A}_k and \mathbf{S}_k are related by the matrix equation

$$\mathbf{A}_k = (\mathbf{U}_k \otimes \dots \otimes \mathbf{U}_1) \mathbf{S}_k (\mathbf{U}_d \otimes \dots \otimes \mathbf{U}_{k+1})^\top,$$

where \otimes denotes the matrix Kronecker product.

For $\mathbf{A} \in \mathbb{C}^{m \times n}$ and $\mathbf{B} \in \mathbb{C}^{p \times q}$, the Kronecker product $\mathbf{A} \otimes \mathbf{B}$ is the $mp \times nq$ block matrix

$$\mathbf{A} \otimes \mathbf{B} = \begin{bmatrix} a_{11} \mathbf{B} & \dots & a_{1n} \mathbf{B} \\ \vdots & \ddots & \vdots \\ a_{m1} \mathbf{B} & \dots & a_{mn} \mathbf{B} \end{bmatrix}.$$

Proposition II.2 ([13]). Let $\mathbf{A} \in \mathbb{R}^{m \times n}$, $\mathbf{B} \in \mathbb{R}^{p \times q}$, $\mathbf{C} \in \mathbb{R}^{n \times l}$, and $\mathbf{D} \in \mathbb{R}^{q \times r}$. Then $(\mathbf{A} \otimes \mathbf{B})^\top = \mathbf{A}^\top \otimes \mathbf{B}^\top$, and $(\mathbf{A} \otimes \mathbf{B})(\mathbf{C} \otimes \mathbf{D}) = (\mathbf{A}\mathbf{C}) \otimes (\mathbf{B}\mathbf{D})$.

B. UTV decomposition

For the matrix $\mathbf{A} \in \mathbb{R}^{m \times n}$, its UTV decomposition takes the form $\mathbf{A} = \mathbf{U}\mathbf{T}\mathbf{V}^\top$, where $\mathbf{U} \in \mathbb{R}^{m \times n}$ and $\mathbf{V} \in \mathbb{R}^{n \times n}$ have orthonormal columns, and \mathbf{T} is a triangular matrix. There are two different cases of UTV decomposition corresponding to the structure of the matrix \mathbf{T} .

If the middle matrix \mathbf{T} is upper-triangular, then the decomposition called URV decomposition, which takes the form

$$\mathbf{A} = \mathbf{U} \begin{bmatrix} \mathbf{R}_{11} & \mathbf{R}_{12} \\ \mathbf{O}_{(m-r) \times r} & \mathbf{R}_{22} \end{bmatrix} \mathbf{V}^\top, \quad (3)$$

where $\mathbf{R}_{11} \in \mathbb{R}^{r \times r}$, $\mathbf{R}_{22} \in \mathbb{R}^{(m-r) \times (n-r)}$ are upper triangular, \mathbf{O} denotes the zero matrix whose elements are all 0, and $\mathbf{R}_{12} \in \mathbb{R}^{r \times (n-r)}$ with small entries. Moreover, suppose the numerical rank of \mathbf{A} is r , then the UTV decomposition is said to be rank-revealing if

$$\sigma_{\min}(\mathbf{R}_{11}) = O(\sigma_r) \quad \text{and} \quad \|\begin{bmatrix} \mathbf{R}_{12}^\top & \mathbf{R}_{22}^\top \end{bmatrix}\|_2 = O(\sigma_{r+1}), \quad (4)$$

where σ_r is the r th largest singular value of \mathbf{A} .

If \mathbf{T} is lower triangular, the decomposition is called ULV decomposition:

$$\mathbf{A} = \mathbf{U} \begin{bmatrix} \mathbf{L}_{11} & \mathbf{O}_{r \times (n-r)} \\ \mathbf{L}_{21} & \mathbf{L}_{22} \end{bmatrix} \mathbf{V}^\top, \quad (5)$$

here \mathbf{L}_{11} and \mathbf{L}_{22} are lower triangular, $\mathbf{L}_{21} \in \mathbb{R}^{(m-r) \times r}$, and the ULV decomposition is said to be rank-revealing if

$$\sigma_{\min}(\mathbf{L}_{11}) = O(\sigma_r) \quad \text{and} \quad \|\begin{bmatrix} \mathbf{L}_{21} & \mathbf{L}_{22} \end{bmatrix}\|_2 = O(\sigma_{r+1}). \quad (6)$$

The smaller the norm of the off-diagonal block, the better the truncated low-rank approximations in (4) and (6). In fact, the UTV decomposition of a matrix is not unique, and various matrix decompositions proposed in the literature can be regarded as UTV-type, such as the rank-revealing QR decomposition [3], the pivoted QLP decomposition [37], and the SVD is also a special case of UTV decomposition when the middle matrix is diagonal. There are a lot of efficient algorithms for UTV decomposition. Stewart [36] introduced the algorithms for UTV decomposition that are well-suited for high-rank matrices. Fierro *et al.* [12], [10] proposed the low-rank UTV algorithms and built up a Matlab package named ‘UTV Tools’ for efficient rank-revealing decompositions. In recent years, more fast randomized algorithms are proposed for UTV decomposition which are flexible for parallel processing in modern architectures [26], [22], [16]. In many practical applications, they can achieve comparable accuracy at a lower computational cost than the classical SVD.

III. TT-UTV ALGORITHMS

In this section, we propose the TT-UTV algorithms for computing the approximate TT-format by sequentially separating the cores by the UTV decompositions, and demonstrate their feasibility through theoretical analysis.

A. TT-ULV case

If the required TT-ranks are fixed, the TT-ULV algorithm is shown in Algorithm 1, which computes the approximate TT-format tensor with left-orthogonal cores in a left-to-right sweep.

Algorithm 1 TT-ULV algorithm for fixed TT-ranks (left-to-right sweep)

Input: d -dimensional tensor $\mathcal{A} \in \mathbb{R}^{I_1 \times \dots \times I_d}$, fixed TT-ranks $\{r_0, r_1, \dots, r_d\}$ with $r_0 = r_d = 1$.

Output: Left-orthogonal TT-cores $\mathcal{G}^{(1)}, \dots, \mathcal{G}^{(d)}$ of the approximation $\hat{\mathcal{A}}$ with TT-ranks r_k 's.

- 1: Temporary matrix: $\mathbf{C} = \text{reshape}(\mathcal{A}, [I_1, I_2 \dots I_d])$, i.e., the first unfolding matrix \mathbf{A}_1 .
 - 2: for $k = 1$ to $d - 1$ do
 - 3: $\mathbf{C} := \text{reshape}(\mathbf{C}, [r_{k-1}I_k, I_{k+1} \dots I_d])$.
 - 4: Compute the truncated rank- r_k approximation from ULV decomposition $\mathbf{C} = \hat{\mathbf{U}}\hat{\mathbf{L}}\hat{\mathbf{V}}^\top + \mathbf{E}$, where $\hat{\mathbf{U}}\hat{\mathbf{L}}\hat{\mathbf{V}}^\top$ with $\hat{\mathbf{L}} \in \mathbb{R}^{r_k \times r_k}$ is the leading term and \mathbf{E} denotes the residual part in the ULV decomposition (5).
 - 5: New core: $\mathcal{G}^{(k)} = \text{reshape}(\mathbf{U}_1, [r_{k-1}, I_k, r_k])$.
 - 6: $\mathbf{C} = \hat{\mathbf{L}}\hat{\mathbf{V}}^\top$.
 - 7: end for
 - 8: $\mathcal{G}^{(d)} = \mathbf{C}$.
-

To facilitate the presentation of error analysis, we introduce some notations. The TT-ULV algorithm 1 adopts

the left-to-right sweep (steps 2-7). In the k th iteration, step 3 computes a temporary matrix $\mathbf{C} \in \mathbb{R}^{r_{k-1}I_k \times I_{k+1} \dots I_d}$, we denote its corresponding $(d - k + 2)$ th-order tensor by $\mathcal{A}^{(k)} = \text{reshape}(\mathbf{C}, [r_{k-1}, I_k, I_{k+1}, \dots, I_d]) \in \mathbb{R}^{r_{k-1} \times I_k \times \dots \times I_d}$, and the $(d - k + 1)$ th-order tensor by $\tilde{\mathcal{A}}^{(k)} = \text{reshape}(\mathbf{C}, [r_{k-1}I_k, I_{k+1}, \dots, I_d]) \in \mathbb{R}^{r_{k-1} \times I_k \times I_{k+1} \times \dots \times I_d}$. Step 4 computes the column-orthogonal matrix $\hat{\mathbf{U}} \in \mathbb{R}^{r_{k-1}I_k \times r_k}$, denoted by $\mathbf{U}^{(k)}$ in the k th iteration. The whole computational processes generate temporary tensors $\{\mathcal{A}^{(k)}\}_{k=1}^{d-1}$, $\{\tilde{\mathcal{A}}^{(k)}\}_{k=1}^{d-1}$, and $d - 1$ column-orthogonal matrices $\{\mathbf{U}^{(k)}\}_{k=1}^{d-1}$ that give birth to the TT-cores. We firstly derive the following proposition and lemma.

Proposition III.1. *The unfolding matrices of tensors $\{\mathcal{A}^{(k)}\}_{k=1}^{d-1}$ satisfy the following equations*

$$\mathbf{A}_l^{(k+1)} = \left(\mathbf{I}_{I_{k+l-1}} \otimes \dots \otimes \mathbf{I}_{I_{k+1}} \otimes \mathbf{U}^{(k)\top} \right) \mathbf{A}_{l+1}^{(k)}, \quad (7)$$

for $l = 1, \dots, d - k + 1$ for all $k = 1, \dots, d - 1$, where $\mathbf{A}_l^{(k)}$ is the l th unfolding matrix of tensor $\mathcal{A}^{(k)} \in \mathbb{R}^{r_{k-1} \times I_k \times \dots \times I_d}$, $\mathbf{I}_m \in \mathbb{R}^{m \times m}$ is the identity matrix, and \otimes denotes the matrix Kronecker product.

Proof. In the k th iteration of the TT-ULV algorithm 1, the rank- r_k truncated ULV decomposition in step 4 can be written as

$$\mathbf{A}_2^{(k)} = \mathbf{U}^{(k)} \mathbf{A}_1^{(k+1)} + \mathbf{E},$$

where $\mathbf{A}_2^{(k)} \in \mathbb{R}^{r_{k-1}I_k \times I_{k+1} \dots I_d}$, $\mathbf{U}^{(k)} \in \mathbb{R}^{r_{k-1}I_k \times r_k}$, $\mathbf{A}_1^{(k+1)} \in \mathbb{R}^{r_k \times I_{k+1} \dots I_d}$. From the orthogonality $\mathbf{U}^{(k)\top} \mathbf{E} = \mathbf{O}$,

$$\mathbf{A}_1^{(k+1)} = \mathbf{U}^{(k)\top} \mathbf{A}_2^{(k)}. \quad (8)$$

From the definitions of the notations $\mathcal{A}^{(k)}$ and $\tilde{\mathcal{A}}^{(k)}$, the l th unfolding matrices of $\tilde{\mathcal{A}}^{(k)}$ are exactly the $(l + 1)$ th unfolding matrix of $\mathcal{A}^{(k)}$, i.e., $\mathbf{A}_{l+1}^{(k)}$, for $l = 1, \dots, d - k + 1$. Clearly, the above equation (8) can be rewritten as the tensor format

$$\mathcal{A}^{(k+1)} = \tilde{\mathcal{A}}^{(k)} \times_1 \mathbf{U}^{(k)\top} \times \mathbf{I}_{I_{k+1}} \times \dots \times \mathbf{I}_{I_d}.$$

From the above tensor equation, the equations (7) hold by Proposition 2.1. \square

Lemma III.1. *Let $m \geq s \geq r$ be positive integers, $\mathbf{Q} \in \mathbb{R}^{s \times m}$ with $\mathbf{Q}\mathbf{Q}^\top = \mathbf{I}_s$, $\mathbf{A} \in \mathbb{R}^{m \times n}$, and $\mathbf{B} = \mathbf{Q}\mathbf{A} \in \mathbb{R}^{s \times n}$. Then the rank- r truncated error of the ULV (or URV) decomposition of \mathbf{B} can be smaller than that of \mathbf{A} .*

Proof. Suppose a rank- r truncated ULV decomposition of \mathbf{A} is

$$\mathbf{A} = \hat{\mathbf{U}}\hat{\mathbf{L}}\hat{\mathbf{V}}^\top + \mathbf{E},$$

and the truncated error $\|\mathbf{E}\|_F = \varepsilon$, where $\hat{\mathbf{U}} \in \mathbb{R}^{m \times r}$. Then

$$\mathbf{B} = \mathbf{Q}\hat{\mathbf{U}}\hat{\mathbf{L}}\hat{\mathbf{V}}^\top + \mathbf{Q}\mathbf{E}.$$

Since \mathbf{Q} has orthogonal rows with unit norm, $\|\mathbf{Q}\|_2 = 1$, $\|\mathbf{Q}\mathbf{E}\|_F \leq \|\mathbf{E}\|_F$. For $\mathbf{Q}\hat{\mathbf{U}} \in \mathbb{R}^{s \times r}$, we can perform the Gram-Schmidt orthogonalization process to its columns to obtain a decomposition (similar to the QR decomposition) $\mathbf{Q}\hat{\mathbf{U}} = \tilde{\mathbf{U}}\tilde{\mathbf{L}}$, where $\tilde{\mathbf{U}} \in \mathbb{R}^{s \times r}$ has orthogonal columns with

unit norm and $\mathbf{L} \in \mathbb{R}^{r \times r}$ is lower-triangular. Then $\tilde{\mathbf{L}} = \widehat{\mathbf{L}}\mathbf{L}$ is still a lower-triangular matrix. Therefore,

$$\mathbf{B} = \tilde{\mathbf{U}}\tilde{\mathbf{L}}\widehat{\mathbf{V}}^\top + \mathbf{Q}\mathbf{E},$$

the leading term $\tilde{\mathbf{U}}\tilde{\mathbf{L}}\widehat{\mathbf{V}}^\top$ is actually a rank- r truncated ULV decomposition of \mathbf{B} . Thus, it finds a rank- r truncated ULV decomposition for \mathbf{B} such that the approximate error $\|\mathbf{Q}\mathbf{E}\|_F$ is smaller than that of \mathbf{A} . For the URV case, the above analysis similarly holds. \square

Remark III.1. From the properties of the Kronecker product, it is easily verified that the Kronecker matrices $(\mathbf{I}_{I_{k+l-1}} \otimes \cdots \otimes \mathbf{I}_{I_{k+1}} \otimes \mathbf{U}^{(k)\top})$ in the equation (7) are row-orthogonal with unit-norm rows.

Next, based on Proposition III.1 and Lemma III.1 the error analysis for the TT-ULV algorithm 1 can be derived, which can be seen as the generalizations of the results for TT-SVD [29].

Theorem III.1 (TT-ULV case). Given a tensor $\mathcal{A} \in \mathbb{R}^{I_1 \times \cdots \times I_d}$. Assume that the rank- r_k approximation error of its k th unfolding matrix $\mathbf{A}_k \in \mathbb{R}^{(I_1 \cdots I_k) \times (I_{k+1} \cdots I_d)}$ from the ULV decomposition (5) is ε_k , that is,

$$\mathbf{A}_k = \mathbf{U}_1^{(k)} \mathbf{L}_{11}^{(k)} \mathbf{V}_1^{(k)\top} + \mathbf{E}^{(k)},$$

where $\mathbf{L}_{11}^{(k)} \in \mathbb{R}^{r_k \times r_k}$, $\mathbf{E}^{(k)} = \mathbf{U}_2^{(k)} (\mathbf{L}_{21}^{(k)} \mathbf{V}_1^{(k)\top} + \mathbf{L}_{22}^{(k)} \mathbf{V}_2^{(k)\top})$ and $\|\mathbf{E}^{(k)}\|_F = \varepsilon_k$ for all $k = 1, \dots, d-1$. Then the approximate tensor $\hat{\mathcal{A}}$ with TT-ranks not higher than r_k 's, computed via TT-ULV algorithm 1 in the left-to-right sweep, meets

$$\|\mathcal{A} - \hat{\mathcal{A}}\|_F \leq \sqrt{\sum_{k=1}^{d-1} \varepsilon_k^2}. \quad (9)$$

Proof. It yields the first TT-core from the ULV decomposition of the first unfolding matrix

$$\mathbf{A}_1 = \mathbf{U}_1^{(1)} \mathbf{A}_2^{(2)} + \mathbf{E}^{(1)}, \quad (10)$$

where $\mathbf{U}_1^{(1)} \in \mathbb{R}^{I_1 \times r_1}$ leads to the first TT-core, and $\mathbf{A}_2^{(2)} = \mathbf{L}_{11}^{(1)} \mathbf{V}_1^{(1)\top} \in \mathbb{R}^{r_1 \times (I_2 \cdots I_d)}$ is used to produce the subsequent TT-cores. Based on the column orthogonality, it follows that $\mathbf{U}_1^{(1)\top} \mathbf{E}^{(1)} = \mathbf{O}$. As we can see, the subsequent processes are to approximate the $(d-1)$ th-order tensor $\tilde{\mathcal{A}}^{(2)} = \text{reshape}(\mathbf{A}_2^{(2)}, [r_1 I_2, I_3, \dots, I_d])$ folded from the matrix $\mathbf{A}_2^{(2)}$. We denote by $\mathcal{B} \in \mathbb{R}^{r_1 I_2 \times I_3 \times \cdots \times I_d}$ the approximation of $\tilde{\mathcal{A}}^{(2)}$ computed by the algorithm, and $\mathbf{B} = \text{reshape}(\mathcal{B}, [r_1, (I_2 \cdots I_d)])$. Then the approximate error of the output tensor $\hat{\mathcal{A}}$ of the TT-ULV algorithm is

$$\begin{aligned} \|\mathcal{A} - \hat{\mathcal{A}}\|_F^2 &= \|\mathbf{A}_1 - \mathbf{U}_1^{(1)} \mathbf{B}\|_F^2 \\ &= \|\mathbf{A}_1 - \mathbf{U}_1^{(1)} \mathbf{A}_2^{(2)} + \mathbf{U}_1^{(1)} \mathbf{A}_2^{(2)} - \mathbf{U}_1^{(1)} \mathbf{B}\|_F^2 \\ &\leq \|\mathbf{E}^{(1)}\|_F^2 + \|\mathbf{A}_2^{(2)} - \mathbf{B}\|_F^2 \\ &= \varepsilon_1^2 + \|\tilde{\mathcal{A}}^{(2)} - \mathcal{B}\|_F^2, \end{aligned} \quad (11)$$

where the third inequality is from the orthogonality of $\mathbf{U}_1^{(1)\top} \mathbf{E}^{(1)} = \mathbf{O}$ and $\|\mathbf{U}_1^{(1)}\|_2 = 1$. Therefore, it reduces to the estimation of the approximate error for the $(d-1)$ th-order

tensor $\tilde{\mathcal{A}}^{(2)}$ by TT-ULV algorithm. As explained in Proposition III.1, Lemma III.1 and Remark III.1, the the truncated error of rank- r_k approximation from the ULV decomposition of the $(k-1)$ th unfolding matrix of $\tilde{\mathcal{A}}^{(2)}$ can be smaller than the approximate error ε_k of the rank- r_k truncated ULV decomposition for \mathbf{A}_k , for all $k = 1, \dots, d-1$. Hence, Based on the above analysis and mathematical induction method, we get

$$\|\tilde{\mathcal{A}}_2 - \mathcal{B}\|_F^2 \leq \sum_{k=2}^{d-1} \varepsilon_k^2.$$

Combine it with the equation (11), the theorem is proved. \square

From the analysis of Theorem III.1, we can also bound the total approximate error of the TT-UTV algorithm 1 by the local errors of each step in the truncated UTV decompositions.

Corollary III.1. For the TT-ULV algorithm 1 in the left-to-right sweep, if the error of the k th truncated ULV decomposition in step 4 is δ_k , then the total error of the computed TT-approximation tensor $\hat{\mathcal{A}}$ satisfies $\|\mathcal{A} - \hat{\mathcal{A}}\|_F \leq \sqrt{\sum_{k=1}^{d-1} \delta_k^2}$.

Therefore, the version of the TT-ULV algorithm in the left-to-right sweep for prescribed accuracy can be easily formulated by referring to Algorithm 1 and the TT-SVD [29, Algorithm 1].

Algorithm 2 TT-ULV algorithm for prescribed accuracy (left-to-right sweep)

Input: A d -dimensional tensor \mathcal{A} , prescribed relative error ε .

Output: Left-orthogonal TT-cores $\mathcal{G}^{(1)}, \dots, \mathcal{G}^{(d)}$ of the approximation tensor $\hat{\mathcal{A}}$ with TT-ranks r_k not higher than the ULV truncated ranks of the unfolding matrices \mathbf{A}_k such that the error $\delta = \frac{\varepsilon}{\sqrt{d-1}} \|\mathcal{A}\|_F$. Then the computed approximation satisfies

$$\|\mathcal{A} - \hat{\mathcal{A}}\|_F \leq \varepsilon \|\mathcal{A}\|_F.$$

- 1: Compute truncation parameter $\delta = \frac{\varepsilon}{\sqrt{d-1}} \|\mathcal{A}\|_F$, set $r_0 = 1$.
 - 2: Temporary matrix: $\mathbf{C} = \text{reshape}(\mathcal{A}, [I_1, I_2 \cdots I_d])$.
 - 3: for $k = 1$ to $d-1$ do
 - 4: $\mathbf{C} := \text{reshape}(\mathbf{C}, [r_{k-1} I_k, I_{k+1} \cdots I_d])$.
 - 5: Compute δ -truncated ULV decomposition $\mathbf{C} = \widehat{\mathbf{U}}\widehat{\mathbf{L}}\widehat{\mathbf{V}}^\top + \mathbf{E}$, $\|\mathbf{E}\|_F \leq \delta$, $\widehat{\mathbf{L}} \in \mathbb{R}^{r_k \times r_k}$.
 - 6: New core: $\mathcal{G}^{(k)} := \text{reshape}(\widehat{\mathbf{U}}, [r_{k-1}, I_k, r_k])$.
 - 7: $\mathbf{C} := \widehat{\mathbf{L}}\widehat{\mathbf{V}}^\top$.
 - 8: end for
 - 9: $\mathcal{G}^{(d)} = \mathbf{C}$.
-

An essential requisite for the above error analysis for Algorithm 1 is that in each iteration the column-orthogonal matrices $\widehat{\mathbf{U}}$ used to generate the TT-cores are orthogonal to the residual part \mathbf{E} . Then the accumulation of the truncated errors can be theoretically controlled by a sharp bound (9).

However, if the right-orthogonal TT-cores are needed, the TT-ULV algorithm is theoretically not recommended to be employed in the right-to-left sweep, especially for the computations of the approximate TT tensor under a prescribed accuracy. Since the column-orthogonal matrix $\widehat{\mathbf{V}}$ in truncated

ULV decomposition is not orthogonal to \mathbf{E} , the above analysis for approximate error is no longer valid, and only a larger error bound can be obtained. More details can be seen in the APPENDIX. Interestingly, the URV case is precisely the opposite.

B. TT-URV case

For the URV decomposition (3), the matrix \mathbf{V}_1 is orthogonal to the residual part $(\mathbf{U}_1\mathbf{R}_{12} + \mathbf{U}_2\mathbf{R}_{22})\mathbf{V}_2^\top$. Wherefore, using the URV decomposition in the right-to-left sweep to compute TT format is more suitable. Algorithm 3 presents the TT-URV algorithm for fixed TT-ranks in the right-to-left sweep to compute the TT-format tensor with right-orthogonal cores.

The results similar to Proposition III.1 and Theorem III.1 also hold for Algorithm 3.

Algorithm 3 TT-URV algorithm for fixed TT-ranks (right-to-left sweep)

Input: A d -dimensional tensor $\mathcal{A} \in \mathbb{R}^{I_1 \times \dots \times I_d}$, fixed TT-ranks $\{r_0, r_1, \dots, r_d\}$ with $r_0 = r_d = 1$.

Output: Right-orthogonal TT-cores $\mathcal{G}^{(1)}, \dots, \mathcal{G}^{(d)}$ of the approximation $\hat{\mathcal{A}}$ with TT-ranks r_k 's.

- 1: Temporary matrix: $\mathbf{C} = \text{reshape}(\mathcal{A}, [I_1 \dots I_{d-1}, I_d])$, i.e., the $(d-1)$ th unfolding matrix \mathbf{A}_{d-1} .
 - 2: for $k = d$ to 2 do
 - 3: $\mathbf{C} := \text{reshape}(\mathbf{C}, [I_1 \dots I_{k-1}, I_k r_k])$.
 - 4: Compute the truncated rank- r_{k-1} approximation from URV decomposition $\mathbf{C} = \hat{\mathbf{U}}\hat{\mathbf{R}}\hat{\mathbf{V}}^\top + \mathbf{E}$, where $\hat{\mathbf{U}}\hat{\mathbf{R}}\hat{\mathbf{V}}^\top$ with $\hat{\mathbf{R}} \in \mathbb{R}^{r_{k-1} \times r_{k-1}}$ is the leading term and \mathbf{E} denotes the residual part in the URV decomposition (3).
 - 5: New core: $\mathcal{G}^{(k)} = \text{reshape}(\hat{\mathbf{V}}^\top, [r_{k-1}, I_k, r_k])$.
 - 6: $\mathbf{C} = \hat{\mathbf{U}}\hat{\mathbf{R}}$.
 - 7: end for
 - 8: $\mathcal{G}^{(1)} = \mathbf{C}$.
-

Theorem III.2 (TT-URV case). *Given a tensor $\mathcal{A} \in \mathbb{R}^{I_1 \times \dots \times I_d}$. Assume that the rank- r_k approximation error of its k th unfolding matrix $\mathbf{A}_k \in \mathbb{R}^{(I_1 \dots I_k) \times (I_{k+1} \dots I_d)}$ from the URV decomposition (3) is ε_k , that is,*

$$\begin{aligned} \mathbf{A}_k &= \begin{bmatrix} \mathbf{U}_1^{(k)} & \mathbf{U}_2^{(k)} \end{bmatrix} \begin{bmatrix} \mathbf{R}_{11}^{(k)} & \mathbf{R}_{12}^{(k)} \\ \mathbf{O} & \mathbf{R}_{22}^{(k)} \end{bmatrix} \begin{bmatrix} \mathbf{V}_1^{(k)\top} \\ \mathbf{V}_2^{(k)\top} \end{bmatrix} \\ &= \mathbf{U}_1^{(k)} \mathbf{R}_{11}^{(k)} \mathbf{V}_1^{(k)\top} + \mathbf{E}^{(k)}, \end{aligned}$$

where $\mathbf{R}_{11}^{(k)} \in \mathbb{R}^{r_k \times r_k}$, $\mathbf{E}^{(k)} = (\mathbf{U}_1^{(k)} \mathbf{R}_{12}^{(k)} + \mathbf{U}_2^{(k)} \mathbf{R}_{22}^{(k)}) \mathbf{V}_2^{(k)\top}$ and $\|\mathbf{E}^{(k)}\| = \varepsilon_k$ for all $k = 1, \dots, d-1$. Then the approximate tensor $\hat{\mathcal{A}}$ with TT-ranks not higher than r_k 's, computed via TT-URV algorithm 3 in the right-to-left sweep, meets (9)

Additionally, the TT-URV algorithm for prescribed accuracy employed in the right-to-left sweep can be obtained analogously. We will not repeat it here.

Remark III.2. *Based on the above theoretical analysis, we recommend the TT-ULV algorithm in a left-to-right sweep to*

compute the left-orthogonal TT-cores, and the TT-URV algorithm in a right-to-left sweep to compute the right-orthogonal TT-cores, especially for the computations of the approximate TT tensor under a prescribed accuracy.

IV. NUMERICAL EXPERIMENTS

In this section, we demonstrate the good performances of the TT-UTV algorithms by means of different applications. There are a variety of available algorithms for rank-revealing UTV decomposition, such as the low-rank UTV algorithm [10] packaged in the ‘UTV tools’ [12], [11], which are computationally attractive alternatives to the SVD for low-rank problems. We used them in the following numerical experiments.

A. Discrete multivariate functions

The first example is the Hilbert tensor with elements

$$\mathcal{X}_{i_1 \dots i_d} = \frac{1}{i_1 + \dots + i_d},$$

which possesses low numerical TT-ranks structure [28]. We perform two groups of experiments to test the TT-UTV algorithms, one is on the third-order Hilbert tensor \mathcal{X} of dimensions $160 \times 160 \times 160$, and the TT-ranks are taken as $(1, r, r, 1)$ with $r = 2, 4, \dots, 30$. Figure 1 (a) shows the Frobenius norm errors of the TT approximations obtained by the TT-SVD algorithm in the left-to-right sweep, TT-UTV algorithms 1 and 3, respectively. Table I reports the concrete comparisons of the absolute errors of these algorithms under different TT-ranks, where the term ‘RtoL’ after TT-SVD means the algorithm is executed in the right-to-left sweep, and ‘LtoR’ stands for the left-to-right sweep. It can be seen that the TT decompositions computed by either TT-URV or TT-ULV provide satisfactory accuracy comparable to the TT-SVD.

Another is on the fourth-order Hilbert tensor of dimensions $50 \times 50 \times 50 \times 50$, and its TT-ranks are taken as $(1, r, r, r, 1)$ with $r = 2, 4, \dots, 20$, respectively. Figure 1 (b) shows that the errors decline with the increasing TT-ranks. The errors decrease exponentially as the rank increases, and the three curves are too close to distinguish. All these results show that the TT-UTV algorithms for computing the TT decomposition can provide the same accuracy as the TT-SVD algorithm.

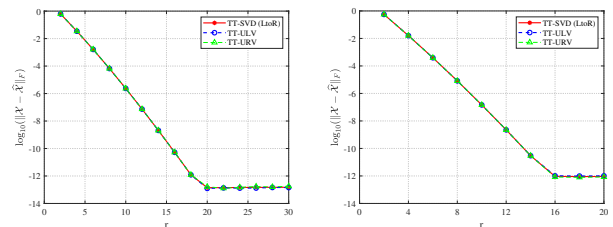


Fig. 1: The logarithms of absolute errors of the TT-approximations \mathcal{X} obtained by various algorithms under different TT-ranks.

TABLE I: Absolute errors of the TT-approximations of the third-order Hilbert tensor

Fixed TT-ranks	(1, 4, 4, 1)	(1, 8, 8, 1)	(1, 12, 12, 1)	(1, 16, 16, 1)	(1, 20, 20, 1)
TT-SVD (LtoR)	3.43803418e-2	6.58860023e-5	7.37806779e-8	5.27161306e-11	1.40761816e-13
TT-ULV	3.43803409e-2	6.58860021e-5	7.37806778e-8	5.27161037e-11	1.24243097e-13
TT-SVD (RtoL)	3.43803418e-2	6.58860023e-5	7.37806779e-8	5.27161314e-11	1.40339130e-13
TT-URV	3.43803410e-2	6.58860021e-5	7.37806779e-8	5.27161611e-11	1.64036599e-13

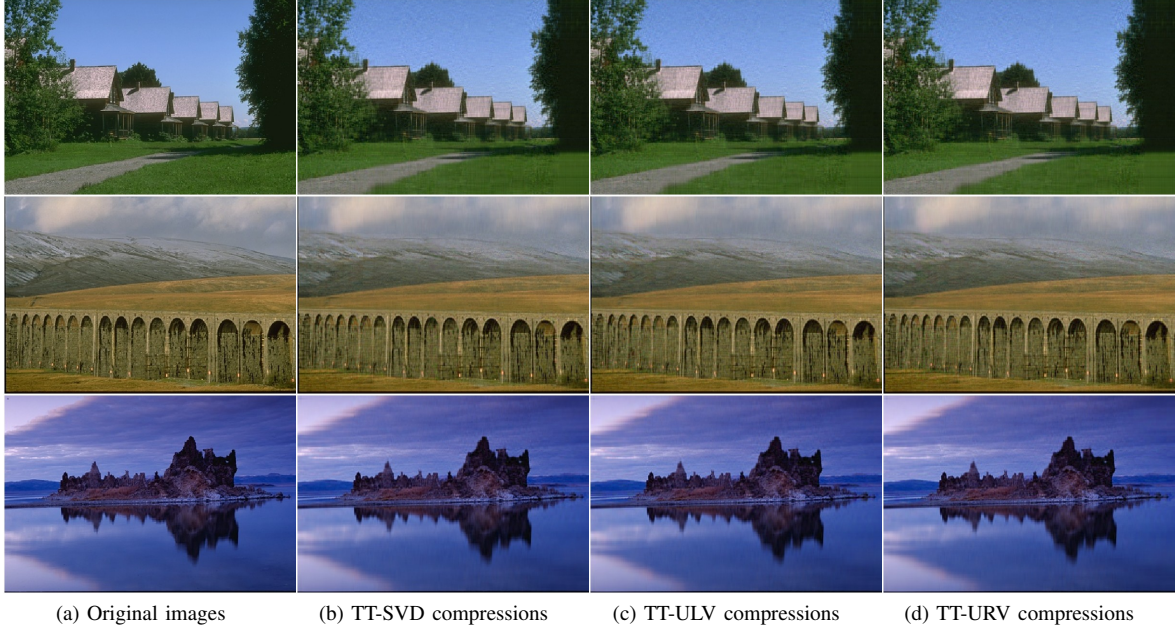


Fig. 2: Color images from the Berkeley Segmentation Dataset.

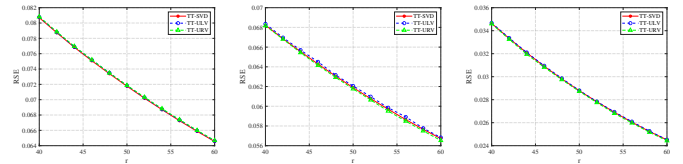
B. Color images

In this experiment, we test the performances of TT-UTV algorithms on image compression. Three color images are picked from the Berkeley Segmentation dataset [25]. In order to facilitate the dimension factorizations, these images are resized into 324×486 dimensions [18] using bicubic interpolation through the MATLAB ‘imresize’ command. Each image is represented by three 324×486 matrices that correspond to the three RGB channels, respectively. For each image, we firstly reshape the channel matrices into higher-order tensors of size $18 \times 18 \times 18 \times 27$, then compute their low-rank approximation by TT-SVD and TT-UTV algorithms.

Figure 2 shows the performances of the TT-compressions on three images, where the TT-ranks are set as $(1, 15, 45, 25, 1)$, hence a TT-compressed image requires only 100035 parameters, much lower than the original image of 472392 parameters. As we can see, these compressed images are too similar to distinguish their resolution and retain most of the information in the original images. Figure 3 reports the relative square errors (RSEs) of the TT-format tensors for these images under different TT-ranks $(1, 15, r, 25, 1)$ with $r = 40, 42, \dots, 60$. The RSEs of the three algorithms are very close.

C. MRI data recovery

When a portion of the information of high-dimensional data is missing or distorted, we can recover the data based on TT-format tensor completion, which can be solved by the Rie-

Fig. 3: The RSEs of the TT compressions of these color images decline with the TT-rank r .

mann gradient descent (RGrad) method [35]. Different from the traditional gradient descent method on Euclidean spaces, RGrad method uses the gradients on Riemannian manifolds formed by the fixed-rank TT-format tensors. From an initial TT-format tensor in the Riemannian manifold, the first step in each iteration is computing the Riemannian gradient $\mathcal{R}\mathcal{G}(\mathcal{X}_k)$ at the current point \mathcal{X}_k . Then compute the estimated tensor $\hat{\mathcal{X}}_{k+1} = \mathcal{X}_k - \alpha_k \mathcal{R}\mathcal{G}(\mathcal{X}_k)$, where α_k is the step size, but it may not locate in the prescribed Riemannian manifold. Hence, the next step is retracting $\hat{\mathcal{X}}_{k+1}$ back to the manifold by the TT-SVD algorithm to generate the next iteration point \mathcal{X}_{k+1} [2], [42]. In this experiment, we explore the effectiveness of the RGrad method while the retracting step in each iteration is substituted by the TT-UTV algorithms.

The experimental results are evaluated by relative square error (RSE) and peak signal-to-noise ratio (PSNR), which are commonly used in the data inpainting tasks [24], [19].

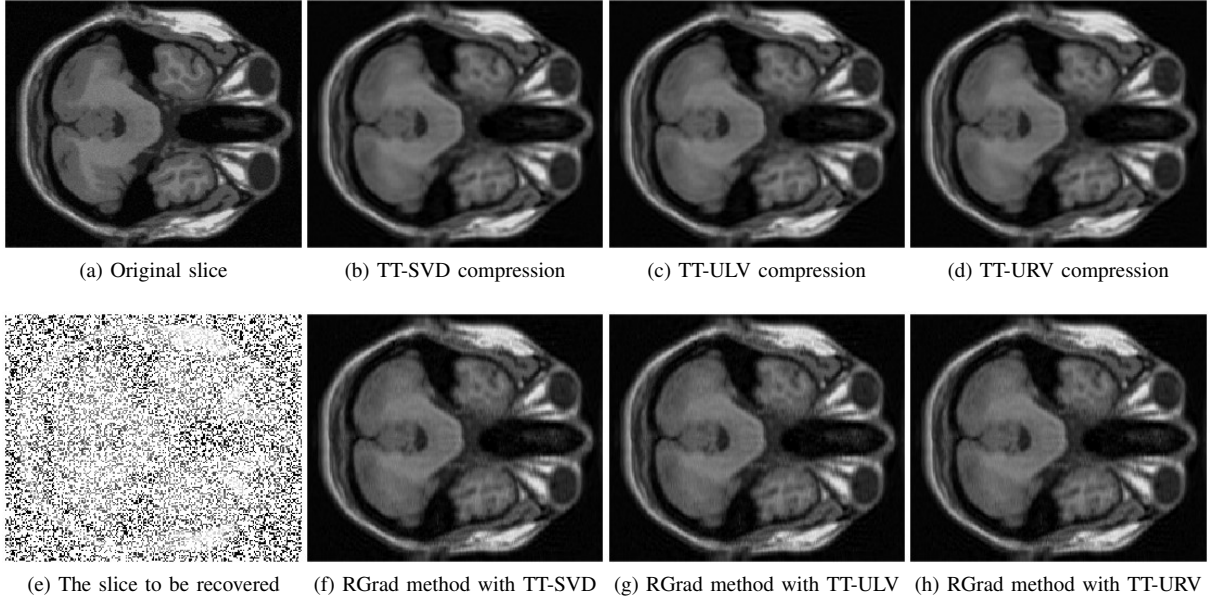


Fig. 4: The reconstruction of one slice $\mathcal{M}_{::36}$ of the MRI data.

Let $\mathcal{M}, \widehat{\mathcal{M}} \in \mathbb{R}^{I_1 \times \dots \times I_d}$ denote the ground-truth tensor and recovered tensor, respectively, then the PSNR is defined as

$$\text{PSNR} = 10 \log_{10} \frac{\mathcal{M}_{max}^2}{\frac{1}{\prod_{k=1}^d I_k} \|\widehat{\mathcal{M}} - \mathcal{M}\|_F^2},$$

where \mathcal{M}_{max} is the maximum value in the ground-truth tensor \mathcal{M} . Smaller RSE and larger PSNR indicate better recovery performance.

We use the cubical MRI data ¹, which is a third-order tensor denoted by \mathcal{M} of size $181 \times 217 \times 181$. Firstly, we determine the truncated TT-ranks of this tensor for the Riemannian manifold. The TT-SVD and TT-UTV algorithms for the prescribed relative error $\varepsilon = 0.1$ all produce the approximate tensors in the TT format with TT-ranks equal to $(1, 55, 41, 1)$. We choose a slice $\mathcal{M}_{::36}$ from the MRI data shown in Figure 4, the four subfigures in the first line present the original slice and compressed ones via various TT decomposition algorithms. As we can see, these compressed slices preserve the most information in the original tensors.

Afterwards, to test the effectiveness of the RGrad method with TT-UTV algorithms, the 70% elements of the original MRI data $\mathcal{M} \in \mathbb{R}^{181 \times 217 \times 181}$ are randomly removed and we would like to recover it. We perform three experiments by the RGrad method where the retracting steps are computed by TT-SVD, TT-ULV, and TT-URV algorithms, respectively. The second row in Figure 4 shows the original slice with missing pixels, and the recovered slices by RGrad methods with TT-SVD, TT-ULV, and TT-URV, respectively. These algorithms have good performances and recover most of the missing data of the original tensor. In addition, Figure 5 (a) reports that the RSEs of the recovered tensor decline with the iterations, which converge to a level close to 0.1, and (b) shows the PSNRs increase in the process of restoration. These curves are too

close to distinguish, which illustrates the RGrad method with TT-UTV is as effective as the RGrad method with TT-SVD.

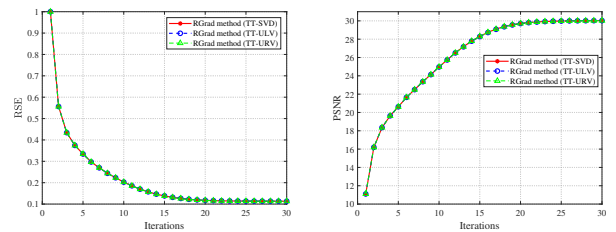


Fig. 5: The RSEs decline and PSNRs increase with the iterations of the RGrad methods with various retracting algorithms.

V. CONCLUSION

In summary, this letter contributes a novel approach called TT-UTV for tensor-train decomposition. It utilizes the virtues of UTV decomposition to compute the TT-format tensors; hence a variety of UTV algorithms can be employed, which require less computational cost than TT-SVD. Through rigorous error analysis, we clarify the effectiveness of these algorithms and the difference between the ULV and URV cases. We recommend the TT-ULV algorithms in a left-to-right sweep to compute the left-orthogonal cores, and the TT-URV algorithm in a right-to-left sweep to compute the right-orthogonal cores. We highlight the efficacy and versatility of the proposed algorithms on image processing and MRI data completion, which can provide comparable accuracy to the TT-SVD.

APPENDIX

The TT-ULV algorithm in the right-to-left sweep is given in Algorithm 4. If the low-rank approximation $\widehat{\mathcal{U}}\widehat{\mathcal{L}}\widehat{\mathcal{V}}$ in step

¹https://brainweb.bic.mni.mcgill.ca/brainweb/selection_normal.html

4 is of size $\widehat{\mathbf{L}} \in \mathbb{R}^{I_1 \cdots I_{k-1} \times r_{k-1}}$ instead of $\widehat{\mathbf{L}} \in \mathbb{R}^{r_{k-1} \times r_{k-1}}$, that is, the two terms $(\mathbf{U}_1 \mathbf{L}_{11} + \mathbf{U}_2 \mathbf{L}_{21}) \mathbf{V}_1^\top$ in the ULV (5), to make the matrix $\widehat{\mathbf{V}} = \mathbf{V}_1$ orthogonal to the residual term $\mathbf{E} = \mathbf{U}_2 \mathbf{L}_{22} \mathbf{V}_2^\top$, then the results similar to Theorem III.1 and Corollary III.1 also hold for the TT-ULV algorithm 4. But it leads to an extra matrix multiplication $\mathbf{U}_2 \mathbf{L}_{21}$ in each iteration.

Algorithm 4 TT-ULV algorithm for fixed TT-ranks (right-to-left sweep)

Input: A d -dimensional tensor $\mathcal{A} \in \mathbb{R}^{I_1 \times \cdots \times I_d}$, fixed TT-ranks $\{r_0, r_1, \dots, r_d\}$ with $r_0 = r_d = 1$.

Output: Right-orthogonal TT-cores $\mathcal{G}^{(1)}, \dots, \mathcal{G}^{(d)}$ of the approximation $\widehat{\mathcal{A}}$ with TT-ranks r_k 's.

- 1: Temporary matrix: $\mathbf{C} = \text{reshape}(\mathcal{A}, [I_1 \cdots I_{d-1}, I_d])$, i.e., the $(d-1)$ th unfolding matrix \mathbf{A}_{d-1} .
- 2: for $k = d$ to 2 do
- 3: $\mathbf{C} := \text{reshape}(\mathbf{C}, [I_1 \cdots I_{k-1}, I_k r_k])$.
- 4: Compute the truncated rank- r_{k-1} approximation from URV decomposition $\mathbf{C} = \widehat{\mathbf{U}} \widehat{\mathbf{L}} \widehat{\mathbf{V}}^\top + \mathbf{E}$, where $\widehat{\mathbf{U}} \widehat{\mathbf{L}} \widehat{\mathbf{V}}^\top$ with $\widehat{\mathbf{L}} \in \mathbb{R}^{r_{k-1} \times r_{k-1}}$ is the leading term and \mathbf{E} denotes the residual part in the ULV decomposition (3).
- 5: New core: $\mathcal{G}^{(k)} = \text{reshape}(\widehat{\mathbf{V}}^\top, [r_{k-1}, I_k, r_k])$.
- 6: $\mathbf{C} = \widehat{\mathbf{U}} \widehat{\mathbf{L}}$.
- 7: end for
- 8: $\mathcal{G}^{(1)} = \mathbf{C}$.

The theory of rank-revealing UTV decomposition tells us that the term $\mathbf{U}_2 \mathbf{L}_{21}$ in (5) can be very minor. Hence, as presented in Algorithm 4, the middle matrix $\widehat{\mathbf{L}}$ of the ULV truncation in step 4 only retains the size $r_{k-1} \times r_{k-1}$ to reduce the computational cost. At the moment, the sharp bound in Corollary III.1 cannot be obtained theoretically for Algorithm 4, but a relatively larger bound can be given by a similar analysis of Theorem III.1 and the triangle inequality of Frobenius norm.

Theorem A.1. *For the TT-ULV algorithm 4 in the right-to-left sweep, if the error of the k th truncated ULV decomposition in step 4 is ε_k , then the total error of the computed TT-approximation tensor $\widehat{\mathcal{A}}$ satisfies*

$$\|\mathcal{A} - \widehat{\mathcal{A}}\|_F \leq \sum_{k=2}^d \varepsilon_k.$$

Based on the above results, as for the TT-ULV algorithm in right-to-left sweep for a prescribed accuracy ε , if the ULV truncation is as step 4 in Algorithm 4, then the truncated error of each ULV decomposition should be $\delta = \frac{\varepsilon}{d-1} \|\mathcal{A}\|_F > \frac{\varepsilon}{\sqrt{d-1}} \|\mathcal{A}\|_F$, which may generate the TT-cores with much higher TT-ranks than the TT-ULV algorithm 2 in the left-to-right sweep. On the other hand, it can also set $\delta = \frac{\varepsilon}{\sqrt{d-1}} \|\mathcal{A}\|_F$, but the middle matrix of ULV truncation $\mathbf{L} \in \mathbb{R}^{I_1 \cdots I_{k-1} \times r_{k-1}}$ should retain a larger size, which leads to more computations. Wherefore, we do not strongly recommend the TT-ULV algorithm for computing right-orthogonal cores by a right-to-left sweep. On the contrary, the TT-URV case is well-suited for computing the right-orthogonal cores in a right-to-left sweep.

REFERENCES

- [1] M. Brazell, N. Li, C. Navasca, and C. Tamon. Solving multilinear systems via tensor inversion. *SIAM Journal on Matrix Analysis and Applications*, 34(2):542–570, 2013.
- [2] J. F. Cai, J. Li, and D. Xia. Provable tensor-train format tensor completion by Riemannian optimization. *Journal of Machine Learning Research*, 23(123):1–77, 2022.
- [3] T. F. Chan. Rank revealing QR factorizations. *Linear Algebra and its Applications*, 88-89:67–82, 1987.
- [4] M. Che and Y. Wei. An efficient algorithm for computing the approximate t-URV and its applications. *Journal of Scientific Computing*, 92(3):93, 2022.
- [5] S. Cui, G. Zhang, H. Jardón-Kojakhmetov, and M. Cao. On discrete-time polynomial dynamical systems on hypergraphs. *IEEE Control Systems Letters*, 2024.
- [6] L. De Lathauwer, B. De Moor, and J. Vandewalle. A multilinear singular value decomposition. *SIAM journal on Matrix Analysis and Applications*, 21(4):1253–1278, 2000.
- [7] J. Demmel, I. Dumitriu, and O. Holtz. Fast linear algebra is stable. *Numerische Mathematik*, 108(1):59–91, 2007.
- [8] S. Dolgov, D. Kalise, and K. K. Kunisch. Tensor decomposition methods for high-dimensional Hamilton–Jacobi–Bellman equations. *SIAM Journal on Scientific Computing*, 43(3):A1625–A1650, 2021.
- [9] R. D. Fierro and J. R. Bunch. Bounding the subspaces from rank revealing two-sided orthogonal decompositions. *SIAM Journal on Matrix Analysis and Applications*, 16(3):743–759, 1995.
- [10] R. D. Fierro and P. C. Hansen. Low-rank revealing UTV decompositions. *Numerical Algorithms*, 15:37–55, 1997.
- [11] R. D. Fierro and P. C. Hansen. UTV expansion pack: Special-purpose rank-revealing algorithms. *Numerical Algorithms*, 40:47–66, 2005.
- [12] R. D. Fierro, P. C. Hansen, and P. S. K. Hansen. UTV tools: Matlab templates for rank-revealing UTV decompositions. *Numerical Algorithms*, 20(2):165–194, 1999.
- [13] G. H. Golub and C. F. Van Loan. *Matrix Computations*. Johns Hopkins University Press, Baltimore, MD, 2013.
- [14] V. Hore, A. Vinuela, A. Buil, J. Knight, M. I. McCarthy, K. Small, and J. Marchini. Tensor decomposition for multiple-tissue gene expression experiments. *Nature Genetics*, 48(9):1094–1100, 2016.
- [15] P. Indyk and R. Motwani. Approximate nearest neighbors: towards removing the curse of dimensionality. In *Proceedings of the Thirtieth Annual ACM Symposium on Theory of Computing*, pages 604–613, 1998.
- [16] M. F. Kaloorazi and J. Chen. Efficient low-rank approximation of matrices based on randomized pivoted decomposition. *IEEE Transactions on Signal Processing*, 68:3575–3589, 2020.
- [17] M. E. Kilmer and C. D. Martin. Factorization strategies for third-order tensors. *Linear Algebra and its Applications*, 435(3):641–658, 2011.
- [18] C.-Y. Ko, K. Batselier, L. Daniel, W. Yu, and N. Wong. Fast and accurate tensor completion with total variation regularized tensor trains. *IEEE Transactions on Image Processing*, 29:6918–6931, 2020.
- [19] C.-Y. Ko, K. Batselier, L. Daniel, W. Yu, and N. Wong. Fast and accurate tensor completion with total variation regularized tensor trains. *IEEE Transactions on Image Processing*, 29:6918 – 6931, 2020.
- [20] T. G. Kolda and B. W. Bader. Tensor decompositions and applications. *SIAM Review*, 51(3):455–500, 2009.
- [21] P. Koniusz, L. Wang, and A. Cherian. Tensor representations for action recognition. *IEEE Transactions on Pattern Analysis and Machine Intelligence*, 44(2):648–665, 2021.
- [22] T. L. Lee, T. Y. Li, and Z. Zeng. RankRev: a Matlab package for computing the numerical rank and updating/downdating. *Numerical Algorithms*, 77:559–576, 2018.
- [23] A. D. Letten and D. B. Stouffer. The mechanistic basis for higher-order interactions and non-additivity in competitive communities. *Ecology Letters*, 22(3):423–436, 2019.
- [24] X. Li, Y. Ye, and X. Xu. Low-rank tensor completion with total variation for visual data inpainting. In *Proceedings of the AAAI Conference on Artificial Intelligence*, volume 31, 2017.
- [25] D. Martin, C. Fowlkes, D. Tal, and J. Malik. A database of human segmented natural images and its application to evaluating segmentation algorithms and measuring ecological statistics. In *Proceedings eighth IEEE international conference on computer vision. ICCV 2001*, volume 2, pages 416–423. IEEE, 2001.
- [26] P. G. Martinsson, G. Quintana-Orti, and N. Heavner. randUTV: A blocked randomized algorithm for computing a rank-revealing UTV factorization. *ACM Transactions on Mathematical Software*, 45(1):1–26, 2019.

- [27] A. Novikov, D. Podoprikin, A. Osokin, and D. P. Vetrov. Tensorizing neural networks. *Advances in Neural Information Processing Systems*, 28, 2015.
- [28] I. Oseledets and E. Tyrtshnikov. TT-cross approximation for multidimensional arrays. *Linear Algebra and its Applications*, 432(1):70–88, 2010.
- [29] I. V. Oseledets. Tensor-train decomposition. *SIAM Journal on Scientific Computing*, 33(5):2295–2317, 2011.
- [30] D. Perez-Garcia, F. Verstraete, M. M. Wolf, and J. I. Cirac. Matrix product state representations. *Quantum Information and Computation*, 7(5):401–430, 2007.
- [31] L. Richter, L. Sallandt, and N. Nüsken. Solving high-dimensional parabolic PDEs using the tensor train format. In *International Conference on Machine Learning*, pages 8998–9009, 2021.
- [32] U. Schollwöck. The density-matrix renormalization group in the age of matrix product states. *Annals of Physics*, 326(1):96–192, 2011.
- [33] F. Sedighin, A. Cichocki, T. Yokota, and et al. Matrix and tensor completion in multiway delay embedded space using tensor train, with application to signal reconstruction. *IEEE Signal Processing Letters*, 27:810–814, 2020.
- [34] N. D. Sidiropoulos, L. De Lathauwer, X. Fu, and et al. Tensor decomposition for signal processing and machine learning. *IEEE Transactions on Signal Processing*, 65(13):3551–3582, 2017.
- [35] M. Steinlechner. Riemannian optimization for high-dimensional tensor completion. *SIAM Journal on Scientific Computing*, 38(5):S461–S484, 2016.
- [36] G. W. Stewart. An updating algorithm for subspace tracking. *IEEE Transactions on Signal Processing*, 40(6):1535–1541, 1992.
- [37] G. W. Stewart. The QLP approximation to the singular value decomposition. *SIAM Journal on Scientific Computing*, 20(4):1336–1348, 1999.
- [38] L. R. Tucker. Some mathematical notes on three-mode factor analysis. *Psychometrika*, 31(3):279–311, 1966.
- [39] M. Vandecappelle and L. De Lathauwer. From multilinear SVD to multilinear UTV decomposition. *Signal Processing*, 198:108575, 2022.
- [40] N. Vannieuwenhoven, R. Vandebril, and K. Meerbergen. A new truncation strategy for the higher-order singular value decomposition. *SIAM Journal on Scientific Computing*, 34(2):A1027–A1052, 2012.
- [41] S. Velasco-Forero and J. Angulo. Classification of hyperspectral images by tensor modeling and additive morphological decomposition. *Pattern Recognition*, 46(2):566–577, 2013.
- [42] J. Wang, G. Zhao, D. Wang, and G. Li. Tensor completion using low-rank tensor train decomposition by riemannian optimization. In *2019 Chinese Automation Congress (CAC)*, pages 3380–3384. IEEE, 2019.
- [43] B. Yang. Projection approximation subspace tracking. *IEEE Transactions on Signal processing*, 43(1):95–107, 1995.
- [44] Y. Yang, D. Krompass, and V. Tresp. Tensor-train recurrent neural networks for video classification. In *International Conference on Machine Learning*, pages 3891–3900. PMLR, 2017.
- [45] M. Zhou and A. J. van der Veen. Stable subspace tracking algorithm based on a signed URV decomposition. *IEEE transactions on signal processing*, 60(6):3036–3051, 2012.